tary crystallographic data for this paper. These data can be obtained free of charge via www.ccdc.cam.ac.uk/conts/retrieving.html (or from the Cambridge Crystallographic Data Centre, 12, Union Road, Cambridge CB2 1EZ, UK; fax: (+44) 1223-336-033; or deposit@ccdc.cam.ac.uk).

[13] a) T. Hayashi, K. Tomioka, O. Yonemitsu, *Asymmetric Synthesis: Graphical Abstracts and Experimental Methods*, Gordon and Breach Science Publishers, Amsterdam, Netherlands, **1998**; b) *Catalytic Asymmetric Synthesis* (Ed.: I. Ojima), VCH, New York, **1993**.

[14] Unit cell parameters for **1c**: orthorhombic, $a = 14.29(2)$, $b = 19.97(4)$, $c = 23.96(4)$ Å, $V = 6834(16)$ Å^3.

Figure 1. A drawing of a $T = 3$ icosadeltahedron—as model for the topologically identical coat protein subunits of the Tomato Bushy Stunt Virus (TBSV)—showing its arrangement of three quasi-equivalent sets of 60 icosahedrally related subunits (lobes/proteins). The orange lobes pack about the icosadeltahedron's exact fivefold axes, whereas the blue and green lobes alternate about its local sixfold axes (reproduced with permission from ref. [3]).

Inorganic Chemistry Goes Protein Size: A Mo_{368} Nano-Hedgehog Initiating Nanochemistry by Symmetry Breaking**

Achim Müller,* Eike Beckmann, Hartmut Bögge, Marc Schmidtmann, and Andreas Dress

Dedicated to Professor Dieter Fenske on the occasion of his 60th birthday

Nature's evolution from the primordial Earth through to the present overwhelming variety of macroscopic forms and functionalities, the formation of which is directed by their molecular "counterparts", that is, by nanosized biomolecules, should stimulate thoughts about the potential of material systems in general as well as related basic first principles or natural laws.[1] We refer to processes based on reservoir systems containing appropriate building blocks, the linking of which can lead to an overwhelming or even infinite variety of molecular forms including those showing symmetry breaking. This process is particularly valid on entering the nanocosmos size category.[2] The nanocosmos as such, does not show the variety-limiting translational symmetry restriction of macroscopic crystalline materials but offers—in contrast to the microcosmos with its small molecules—the possibility that (several) larger arrays with local symmetries are not in agreement with the overall symmetry—a situation well known for spherical viruses (see Figure 1 and ref. [3])—can occur. This increases the options for the generation of an extreme structural versatility. Thus, the appropriate building units must display a certain type of flexibility as prerequisite for linking versatility (of course not coming close to that of amino acids), a condition well fulfilled by molybdenum oxide based fragments/aggregates. These special entities, abundant as (virtual) building units in a potential "dynamic library",[4,5] can, by a type of "split-and-link process", adapt their size and shape depending upon slight alterations of the relevant boundary conditions;[6–8] evident reasons for this "molybdate" specific quality are listed in footnote ref. [9]. This versatility could lead us, to use a term from J.-M. Lehn lectures, to the category "Multiple Expression of Molecular Information", a statement also supported by the variety of giant clusters obtained from relevant "libraries".[6–8] Here we report the formation of a rather unusual giant molybdenum oxide based nanocluster, the size of hemoglobin (diameter approximately 6 nm), and containing 368 metal (1880 non-hydrogen) atoms formed by the linking of 64 $\{Mo_1\}$-, 32 $\{Mo_2\}$-, and 40 $\{Mo(Mo_5)\}$-type units by a remarkable symmetry-breaking process which is nicely recognizable at the cluster surface. The understanding of the present process will be the starting point for the synthesis of quite a number of other "size comparable" clusters and reactions of these. Here we refer to a far-reaching step into the nanocosmos with perspectives for nanochemistry through symmetry breaking, molecular topology, and surface sciences with catalytical and topological relevance. Symmetry breaking will be referred to in relation to transitions from positive to negative surface areas which can be considered as model for nature's patternings or breaking monotony.

By reducing a molybdate solution which is acidified with sulfuric acid, the deep-blue compound **1** containing the giant mixed-valence cluster anion **1a** (Figure 2) is obtained which was characterized by elemental analysis (including redox titrations to determine the (formal) number of Mo^V centers), thermogravimetry (to determine the actual crystal-water content which is important for the analyses), bond valence

[*] Prof. Dr. A. Müller, Dipl.-Chem. E. Beckmann, Dr. H. Bögge, M. Schmidtmann
Lehrstuhl für Anorganische Chemie I
Fakultät für Chemie der Universität
Postfach 100131, 33501 Bielefeld (Germany)
Fax: (+49)521-106-6003
E-mail: a.mueller@uni-bielefeld.de
Prof. Dr. A. Müller, Prof. Dr. A. Dress
Fakultät für Mathematik und Graduiertenkolleg (GK) "Strukturbildungsprozesse", Universität Bielefeld

[**] Financial support by the Deutsche Forschungsgemeinschaft, the Fonds der Chemischen Industrie, the European Union (HPRN-CT 1999-00012) and the GK is gratefully acknowledged.

  1433-7851/02/4107-1162 $ 20.00+.50/0

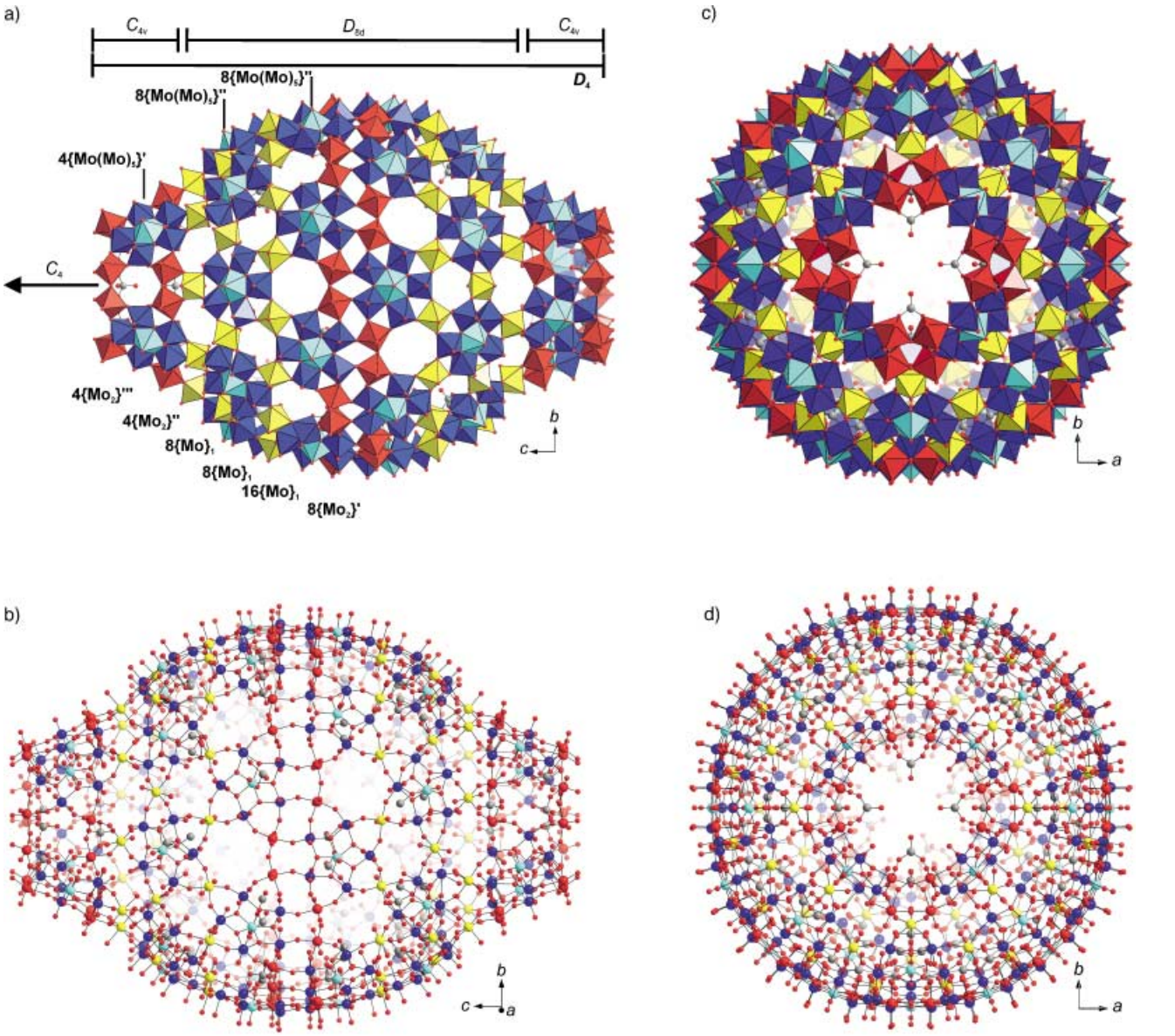

Figure 2. Structure of **1a** in crystals of **1** in polyhedral (a) and ball and stick (b) representation perpendicular to the C_4 axis and along the C_4 axis ((c) and (d); building units {Mo$_1$} yellow, {Mo$_2$} red, {Mo(Mo$_5$)} blue with blue-turquoise pentagonal bipyramids; O atoms small red spheres, S atoms gray spheres). Note that one capping part is turned against the other by 360/16°. The different building blocks and the arrays of different local symmetry are assigned.

sum (BVS) calculations, spectroscopic methods (IR, resonance Raman, Vis/nIR) as well as single-crystal X-ray structure analysis.[10]

$$Na_{48}[H_xMo_{368}O_{1032}(H_2O)_{240}(SO_4)_{48}]\cdot ca.\ 1000\,H_2O \equiv Na_{48}\mathbf{1a}\cdot ca.\ 1000\,H_2O \quad \mathbf{1}$$

$\mathbf{1a} \equiv [H_x\{Mo(Mo_5)\}'_8\{Mo(Mo_5)\}''_{32}\{Mo_2\}'_{16}\{Mo_2\}''_8\{Mo_2\}'''_8\{Mo_1\}_{64}]^{48-}$
$\{Mo(Mo_5)\}' \equiv \{Mo_6O_{21}(H_2O)_6\}$
$\{Mo(Mo_5)\}'' \equiv \{Mo_6O_{21}(H_2O)_3(SO_4)\}$
$\{Mo_2\}' \equiv \{Mo_2O_3(H_2O)_2\}$
$\{Mo_2\}'' \equiv \{Mo_2O(t)_2O(br)_3(SO_4)\}$
$\{Mo_2\}''' \equiv \{Mo_2O(t)_4O(br)(SO_4)\}$
$\{Mo_1\} \equiv \{MoO(H_2O)\}$
$x \approx 16$
(for error limits see ref. [10])

Compound **1** crystallizes in the space group *I*4mm and in the unit cell contains two giant hedgehog-like cluster anions **1a** which have approximate D_4 symmetry with a central ball-shaped fragment $\{Mo_{288}O_{784}(H_2O)_{192}(SO_4)_{32}\}$ (B) and two capping units $\{Mo_{40}O_{124}(H_2O)_{24}(SO_4)_8\}$ (C). Remarkably, there are three rather large areas, that is, two C and one B, with different local symmetries (see Figure 2a): D_{8d} in the central B part and C_{4v} in the two capping areas C. Thus there is a well-defined cross-section where the symmetry breaking occurs and a negative curvature is generated (see Figure 2 and Addendum after Experimental Section).[11, 12] More precisely, **1a** is built up by the six above mentioned well-defined building units (see also Figure 1), while a giant molecular container with a huge cavity (diameter $\approx 2.5 \times 4.0$ nm at its most extended points) is formed offering space, for the tremendously large number of about 400 H_2O molecules. (The number of water molecules in the crystal given above (1000) includes the 400 molecules encapsulated.) The presence of the bidentate SO_4^{2-} ligands (see formulas) can also be shown by

  1433-7851/02/4107-1163 $ 20.00+.50/0

the typical splitting of the $\nu_3(F_2)$-type vibrational bands (1191, 1122, 1060 cm^{-1}), and the abundance of Mo^V as well as Mo^{VI} centers by the IVCT (intervalence charge transfer) band at $\sim$740 nm. The comparably large number of different building units of **1a** can be identified from Figure 2 together with the above given formulas. The two types of $\{Mo(Mo_5)\}$ units differ in the number and coordination type of the SO_4^{2-} ligands: 40 with SO_4^{2-} ligands and eight without located in the C_{4v} areas. The dinuclear units $\{Mo_2\}$ not only differ with respect to the number of bidentate SO_4^{2-} ligands (see formulas) but also, for those at the ends of both C caps, that is, the borderlines, both Mo centers have two terminal O atoms, a situation characteristic for stopping growth. The $\{Mo_1\}$ units are of the classical type $\{OMo^V(H_2O)\}^{3+}$ and contribute correspondingly to the highly reduced state of **1a**. The other formal "Mo^V-type centers" are distributed over several parts of the cluster areas, which causes a widespread delocalization of the Mo 4d electrons.

The structure of **1a** can be considered as a hybrid between the giant wheel ($\{Mo_{176}\}$-type) and ball ($\{Mo_{102}\}$-type) clusters.[7b, 8, 13] We find in **1a** the $\{Mo(Mo_5)\}$ and $\{Mo_1\}$ units of the $\{Mo_{102}\}$ ball-type cluster as well as $\{Mo(Mo_5)\}$ and $\{Mo_2\}$ units of the wheel-type species. The hybrid character is—referring to the terminology of ref. [13]—also manifest by the occurrence of 24 C_5-type $\{Mo_{11}\}$ groups of the ball-type clusters[13] together with the related wheel (same type) 16 C_s-type $\{Mo_{10}\}$ groups with only one MoO_6 octahedron less. Note that the two groups have 56 MoO_6 octahedra in common (Figure 3). Whereas the C_5-$\{Mo_{11}\}$ groups are identical to those of the spherical ball-type clusters,[13] the structure of the $\{Mo_{10}\}$ units of **1a** is identical to that of the $\{Mo_{10}\}$ fragment of the wheel-type cluster C_s-$\{Mo_{11}\}$ unit, which, when compared to the symmetrical ball situation, has only the 11th octahedron displaced.[14]

The high reduction state (ca. 112 Mo^V, 256 Mo^{VI}), which is much higher than that in the wheel systems (e.g., 28 Mo^V, 126 Mo^{VI}[8]), reflects that reducing conditions favor cluster growth. (The largest cluster in acidified molybdate solution is, in absence of a reducing agent, the "rather small" $\{Mo_{36}\}$ anion[15, 16] which "starts growing" upon reduction.[8]) A negative charge or an increase in negative charge does not only prevents uncontrolled linking, but initiates further protonation as a prerequisite for further linking. The negative charge in the present case is supported by the abundance of SO_4^{2-} ligands coordinated to the intermediates and the final cluster species. This situation does not occur in presence of much weaker coordinating ligands, such as Cl^- or ClO_4^- ions: in cases where $HClO_4$ or HCl are used as acidification agents instead of H_2SO_4 not **1a**, but pure molybdenum oxide based wheel-type species are formed.[8] For the present results it is important that the coordination ability of the SO_4^{2-} is not too strong (e.g., as it would be in the case of PO_4^{3-}) thus allowing a flexibility of coordination with the consequence that a variety of different appropriate building blocks can be generated. The average reduction state of the two Mo_{40}-type caps C of **1a** is lower than that of the D_{8d} part B. This observation agrees with our hypothesis that growing processes in POM-type systems are mostly based on nucleophiles which start "growing" by directing the formation of electrophiles (in a relative consideration!) with which they get capped.[17] In the present case, the central B part probably directs the formation of the C type units (see also ref. [18]).

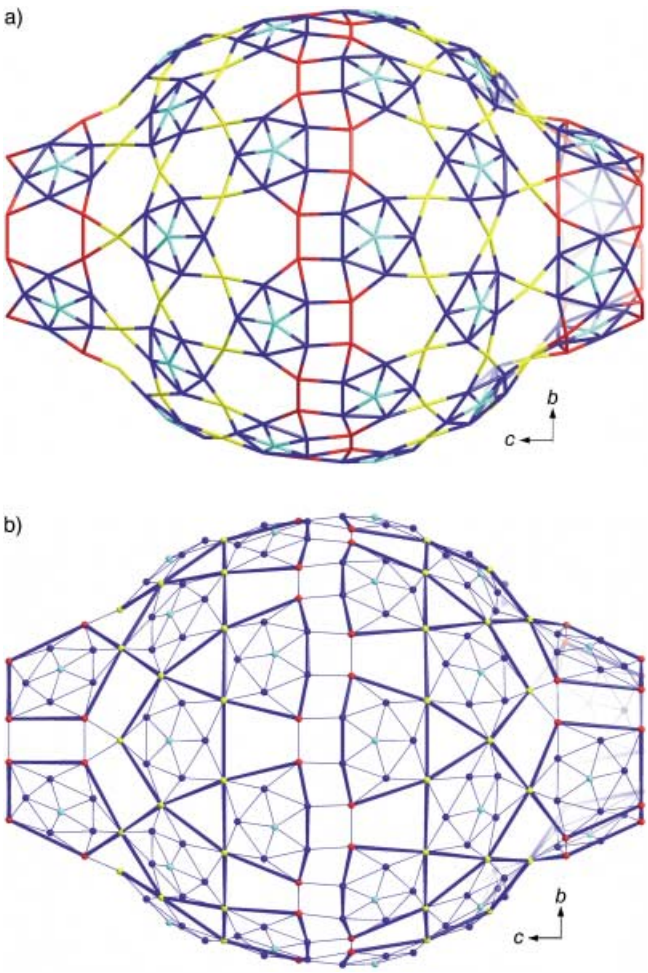

Figure 3. $\{Mo_{368}\}$ metal atom framework of **1a** in wire-frame (a) and in ball and stick representation with $\{Mo_{11}\}$ and $\{Mo_{10}\}$ building blocks emphasized through thick lines (b; color code as in Figure 2).

Our prediction is that the knowledge of structural details of cluster **1a** will be the starting point for the synthesis of many others of comparable size as well as for a new type of nanochemistry which will allow *well defined* reactions to be performed at *well defined* sites of *well defined* nanoobjects, and includes their handling as intact units, for instance for cross-linking or preparation of composites, for example, with silica or surfactants, which is possible with these types of clusters as shown in case of the giant ball- and wheel-type species with the generation of micelles, films, and even liquid crystals.[20] The present results are relevant for catalysis as it is still a challenge to understand details of the interaction mechanisms of substrates with the surfaces of heterogeneous catalysts.[21, 22] In the case of transition metal oxides, such as MoO_3, which play an important role in selective oxidation processes,[22] it would be a tremendous step to consider the surfaces of discrete and well defined giant molybdenum oxide based clusters for model reactions relevant for related catalytically active bulk materials, the surface of which is difficult to investigate[23, 24] (note that the large surface of **1a**

  1433-7851/02/4107-1164 $ 20.00+.50/0

contains only Mo=O and Mo(H_2O) groups). Another interesting aspect is the possibility to perform supramolecular chemistry inside the cavity of the giant molecular container **1a**—the largest structurally well defined one known—as was possible with the smaller ball-type clusters.[7c] Remarkably, this type of nanochemistry/nanotechnology and supramolecular engineering is based on structurally well-defined objects obtained by the "bottom-up" method.[25, 26] Last but not least, the symmetry breaking[11]—"visible" at the surface of **1a** because of the abundance of different large local symmetry areas or negative curvature in between positive curvatures at a giant cluster's surface as in case of Fowler's Phantasmagorical Fulleroids (see Addendum)—has model character for nature's patterning processes in general and, in particular, those occurring within nucleation processes. Symmetry breaking is of fundamental importance for the understanding of patternings in the macroworld (in this respect the antagonistic effect actions are important) which was described by D'Arcy Thompson in his book "*On Growth and Form*"[27c] (for general references see Ref. [11, 27, 28]). In this respect it would be a breakthrough if rather large nanoareas such as B and C with different symmetry could be extended further. In particular, this should be possible under dissipative conditions.

In any case, the formation of **1a** under conservative conditions shows a type of patterning, emergence, and complexity on the nanolevel, though not on the macrolevel, as for instance in case of the dissipative self-organizing model processes leading to Bénard-convection cells and Belousov-Zhabotinsky-type patternings (see ref. [27]). The novelty of the formation of the present nanoobject is that, in spite of its enormous size, a breaking of monotony during growth is observed. This breaking is caused by different distributions of a rather large number of different "negative and positive" vertices with polygons ranging from triangles to heptagons (see Addendum and Figure 4). The complexity here is nicely recognized by comparison with the Archimedean solids having only one type of vertex.

Experimental Section

$Na_2S_2O_4$ (0.15 g, 0.86 mmol) as reducing agent was added to a stirred solution of $Na_2MoO_4 \cdot 2H_2O$ (3 g, 12.4 mmol) in water (10 mL) which was acidified with 0.5 M H_2SO_4 (35 mL; immediate color change to blue). The solution was stored in a closed flask and after 2 weeks the precipitated deep-blue crystals of **1** were collected by filtration, yield: 80 mg (two crystal types: major part showing from top view a characteristic form like an elongated benzene molecule, while a much smaller fraction of the crystals is grown together). Characteristic IR bands (KBr pellet): $\tilde{\nu} = 1616$ (m, δ (H_2O)), 1191 (w), 1122 (w), 1060 (all $\nu_{as}(SO_4)$), 975/954 (s) (ν(Mo=O)), 761 (s), $\approx$700 (sh), 627 (w), 555 (m), 464 (w) cm^{-1}; approximate wavenumbers of the very broad Raman bands (KBr dilution; $\lambda_e = 1064$ nm): $\tilde{\nu} \approx 810$ (m), 680 (w), 460 (m) cm^{-1}; Vis (in H_2O): $\lambda \approx 740$ (very broad) nm.

Addendum

Combinatorial topology of the nanoclusters polyhedral structure relevant for the present surface and symmetry breaking complexity problem: The following section explains first of all the topological nature of the surface of **1a** but could also be of help for the chemist in constructing rather large patterns showing positive and negative curvatures. A combinatorial analysis of the four-regular polyhedral net defined by the Mo atoms of

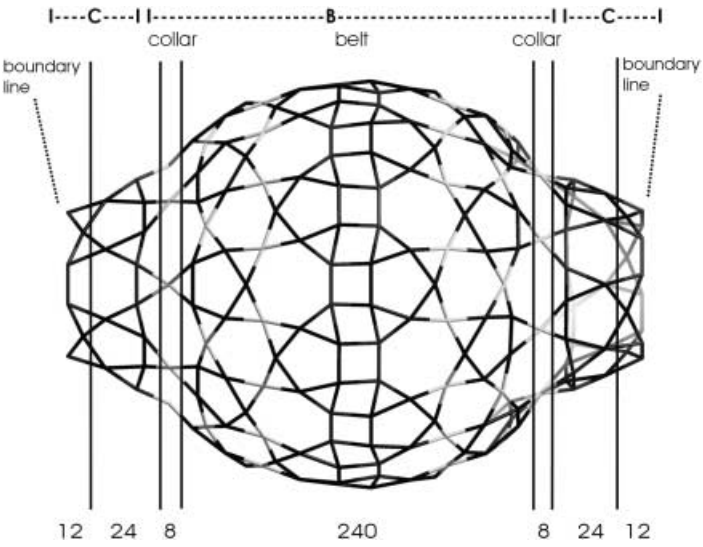

Figure 4. The four-regular polyhedron depicting the surface of **1a**, consisting of 328 = 368 – 40 Mo atoms (i.e. without the Mo atoms of the pentagonal bipyramids); it exhibits 64 vertices in the belt region, 32 with vertex configuration [3,4,4,5], and 32 of type [3,4,4,7], 16 + 8 of type [3,5,3,7], 8 of type [3,5,3,6], and 16 of type [3,6,3,7] in each of the two B regions next to the belt and another two times 16, 8, and 16 of type [3,5,3,6], [3,6,3,7], [3,5,3,7], respectively, next to the two collars, altogether 16 of type [3,7,3,7] along the two collars, and 8 of type [3,6,3,7], [3,5,3,7], and [3,5,3,6] each in the interior of the two capping regions, and 4 of type [3,5,3] and 8 of type [3,6] along each of the two boundary lines.

1a, as shown in Figure 4 (suppressing however, for simplicity, the Mo atoms within the interior of the pentagonal bipyramids) reveals a clear correspondence between the overall distribution of positively and negatively curved surface segments and the distribution of vertices with positive and negative combinatorial curvature. This observation is in agreement with Euler's celebrated theorem[31] interpreted as a discrete version of the equally celebrated Gauss–Bonnet theorem[32] (see Figure 5 and 6 as illustrative examples of positively and negatively curved surfaces).

Indeed, the interior of region B with D_{8d} and of the two capping regions C with C_{4v} symmetry are positively curved; however, these are connected by the two narrow *collars* exhibiting a strong indentation, thus creating two ring-shaped surface components of large negative curvature of relevance for the symmetry breaking. Additional negative curvature is "hidden" in the jaggedness of the two circular boundary lines (indeed, straightening them out into perfect circles would create shapes that would each mimic the shape of a neck, that is, one half of the negatively curved inner part of a torus, see Figure 5). Correspondingly, the average combinatorial curvature (definition in ref. [33]) of the 240 Mo atoms in the interior of B is +4/315 while the same holds for the 48 (24 + 24) Mo atoms in the interior of the two capping regions; in contrast, it is – 30/315 for each of the 16 (8 + 8) Mo atoms in the two collars and – 28/315 for each of the 24 (12 + 12) Mo atoms in the two jagged circular boundary lines.[34] Clearly, this is in perfect agreement with the positive curvature observed in the major parts of B and

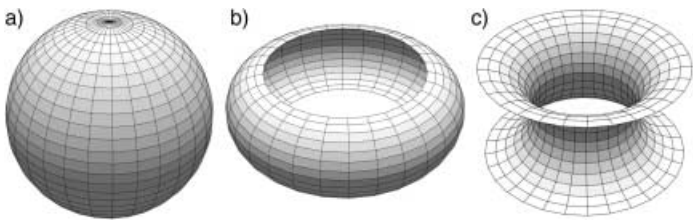

Figure 5. Shapes of positively (a) and (b) and negatively (c) curved surfaces. The sphere and the outer part of a torus are paradigms of surfaces exhibiting positive curvature (a) and (b), the saddle and the inner part of a torus are paradigms of surfaces exhibiting negative curvature (c).

  1433-7851/02/4107-1165 $ 20.00+.50/0

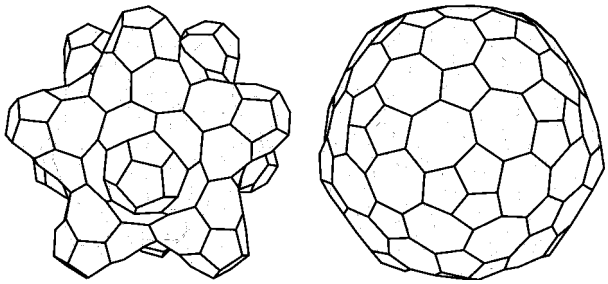

Figure 6. The shown Fowler's Phantasmagorical Fulleroids are text book examples illustrating how areas exhibiting strongly positive curvature can be intertwined with areas exhibiting negative curvature to produce a surface of only moderately positive curvature. Any fulleroid with icosahedral symmmetry consisting of only pentagons and heptagons contains exactly $12+60N$ pentagons and $60N$ heptagons, for some positive integer N. There are two such fulleroids with $N=1$: a) where the 72 pentagons come in 12 clusters of 6 pentagons each generating *outcrops* of high positive curvature counterbalanced by a network of negatively curved *channels* built from its 60 heptagons, which results in a net positive curvature of four as required, b) consisting of 12 single pentagons and 20 clusters of three pentagons each, also connected by a network of negatively curved channels built from the heptagons exhibiting, however, a much smoother geometry because of the much better local balance of positive and negative curvature.

C, being counterbalanced by the considerably stronger negatively curved collars of B and boundary lines of C. Our analysis implies also that, for purely geometric reasons, the nanocluster's shape could not have been built up without the use of, at least, some heptagons counterbalancing the positive curvature implied by the pentagonal building blocks, at least as long as two triangles (or just one triangle and two quadrangles) occur at each interior vertex among the four polygons incident with that vertex (see also Figure 6a). Remarkably, the negative curvature at the two jagged boundary lines of C stops the growth process.

Received: November 15, 2001 [Z18228]

[1] a) J. C. Taylor, *Hidden Unity in Nature's Laws*, Cambridge University Press, Cambridge, **2001**; b) "Was sind und warum gelten Naturgesetze?": *Philosophia Naturalis*, *Vol. 37* (Eds.: P. Mittelstaedt, G. Vollmer), Klostermann, Frankfurt, **2000**, special issue, pp. 189–475, including A. Müller, *Naturgesetzlichkeiten—Chemie lediglich ein Bereich zwischen Physik und biologischem Geschehen?*, pp. 351–365.

[2] The term is usually accepted. See: "Faszinierende Einblicke in den Nanokosmos": K. Schoepe, R. Wiesendanger in … *und Er würfelt doch! Von der Erforschung des ganz Großen, des ganz Kleinen und der ganz vielen Dinge* (Eds.: H. Müller-Krumbhaar, H.-F. Wagner), Wiley-VCH, Weinheim, **2001**, pp. 521–531.

[3] D. Voet, J. G. Voet, *Biochemistry*, 2nd ed., Wiley, New York, **1995**, p. 1082.

[4] For a more general type of dynamic library see also: J.-M. Lehn in *Essays on Contemporary Chemistry, From Molecular Structure towards Biology* (Eds.: G. Quinkert, M. V. Kisakürek), Wiley-VCH, New York, **2001**, pp. 307–326.

[5] Important in this context is that virtual building blocks, e.g. those abundant as fragments of larger units, become available for linking under special boundary conditions. The relevant process is of the category "split and link". An interesting example refers to the important pentagonal unit of the type $\{Mo(Mo_5)\}$ also occurring in **1a**. Its existence within larger fragments was known from many compounds, for instance in those of the $\{Mo_{36}\}$ and $\{Mo_{57}\}$ type[6] and even in extended solid-state structures (N. N. Greenwood, *Ionic Crystals, Lattice Defects and Non Stoichiometry*, Butterworth, London, **1968**). Therefore, the pentagonal unit should also exist as a transferable unit especially because of its high symmetry and because its atoms are densely packed (all polyhedra linked by edges). This finally led to the discovery of the spherical ball system with 12 of these units spanning an icosahedron.[7a] Furthermore, this unit is important for the generation of a large number of nanoclusters with curvatures like the present one (see Addendum).

[6] See: A. Müller, H. Reuter, S. Dillinger, *Angew. Chem.* **1995**, *107*, 2505–2539; *Angew. Chem. Int. Ed. Engl.* **1995**, *34*, 2328–2361, and references therein; see also ref. [15].

[7] a) A. Müller, P. Kögerler, C. Kuhlmann, *Chem. Commun*. **1999**, 1347–1358; b) A. Müller, F. Peters, M. T. Pope, D. Gatteschi, *Chem. Rev.* **1998**, 98, 239–271; c) A. Müller, S. K. Das, P. Kögerler, H. Bögge, M. Schmidtmann, A. X. Trautwein, V. Schünemann, E. Krickemeyer, W. Preetz, *Angew. Chem.* **2000**, *112*, 3555–3559; *Angew. Chem. Int. Ed*. **2000**, *39*, 3413–3417 (see also: *Science* **2000**, *290*, 411).

[8] A. Müller, C. Serain, *Acc. Chem. Res.* **2000**, *33*, 2–10.

[9] Important factors are, the easy change of coordination numbers as well as the easy exchange of H_2O ligands at Mo-sites—not too strong and not too weak Mo-O-Mo-type bonds allowing the "split-and-link" process (these are even "tunable" by alterable boundary conditions, i.e. the reducing conditions)—easy change of electron densities not only within the Mo–O bonds but also at the O sites (important for protonation) depending on the redox conditions which increases the linking versatility of specific groups—no strong tendency to form metal–metal bonds, which limits the structural versatility, as is the case of tungsten—and last but not least, the presence of terminal Mo=O groups protecting unlimited growth to extended structures. Important: we refer here in this context to mixed valence compounds of type III (complete electron delocalization) in the of Robin and Day classification. (The fundamental compound types are discussed e.g. in: "Mixed Valency Systems: Applications in Chemistry, Physics and Biology" (Ed.: K. Prassides), Kluwer, Dordrecht, **1991**.)

[10] Crystal data for **1** $H_{2496}Mo_{368}Na_{48}O_{2464}S_{48}$, $M=79888.16\ g\,mol^{-1}$, tetragonal, space group $I4mm$, $a=43.4648(13)$, $c=69.393(3)$ Å, $V=131097(8)$ Å^3, $Z=2$, $\rho=2.023\ g\,cm^{-3}$, $\mu=1.856\ mm^{-1}$, $F(000)=77920$, crystal size $=0.20\times0.15\times0.10\ mm^3$. Crystals of **1** were removed from the mother liquor and immediately cooled to 163(2) K on a Bruker AXS SMART diffractometer (three circle goniometer with 1 K CCD detector, $Mo_{K\alpha}$ radiation, graphite monochromator; hemisphere data collection in ω at 0.3° scan width in three runs with 606, 435, and 230 frames ($\phi=0$, 88 and 180°) at a detector distance of 5 cm). A total of 211056 reflections ($0.66<\Theta<20.03°$) were collected of which 32441 reflections were unique ($R(\mathrm{int})=0.1326$). An empirical absorption correction using equivalent reflections was performed with the program SADABS. The structure was solved with the program SHELXS-97 and refined using SHELXL-93 to $R=0.0768$ for 23699 reflections with $I>2\sigma(I)$, $R=0.1233$ for all reflections; max./min. residual electron density 1.837 and $-1.490\ e\,Å^{-3}$. (SHELXS/L, SADABS from G. M. Sheldrick, University of Göttingen **1997/93**; structure graphics with DIAMOND 2.1 from K. Brandenburg, Crystal Impact GbR, **2001**.) Further details on the crystal structure investigation may be obtained from the Fachinformationszentrum Karlsruhe, 76344 Eggenstein-Leopoldshafen, Germany (fax: (+49) 7247-808-666; e-mail: crysdata@fiz-karlsruhe.de), on quoting the depository number CSD-412283. The number of "crystal" H_2O molecules of the formula corresponds to the unit cell volume and is the maximum possible number regarding the space left. (This corresponds to our usual procedure as these types of compounds continuously release crystal water as a result of weathering.) The given number of protonations in the formula correlates with the analytically determined values of the (formal) number of Mo^V centers (112), and the found Na value. Whereas these values have a small error limit, the number of SO_4^{2-} ligands could—though they are disordered—be accurately determined according to the excellent agreement between results from elemental analysis and the single-crystal X-ray structure data. The H atoms disordered at (many) sulfate sites cannot be located.

[11] See H. Genz, *Symmetrie und Symmetriebrechung in der Physik*, Vieweg, Braunschweig, **1991**; H. Haken, *Synergetics*, 3rd ed. Springer, Berlin, **1983**; K. Mainzer, *Thinking in Complexity*, 3rd ed., Springer, Berlin, **1997**.

[12] It is logical that the symmetry-breaking-based linking of the arrays B and C, with different local symmetry, occurs by vertices (and not

  1433-7851/02/4107-1166 $ 20.00+.50/0

edges) of related polyhedra because this allows higher flexibility (see also Addendum).
[13] A. Müller, P. Kögerler, H. Bögge, *Struct. Bonding* **2000**, *96*, 203 – 236.
[14] The situation that the ball- ($n = 12$) and wheel-type ($n = 14, 16$) cluster species could be expressed by the same basic type of stoichiometry $\{Mo_{11}\}_n$, that is, only referring to different numbers n, was categorized by us as a Phythagorean harmony.[13]
[15] M. T. Pope, A. Müller, *Angew. Chem.* **1991**, *103*, 56 – 70; *Angew. Chem. Int. Ed. Engl.* **1991**, *30*, 34 – 48.
[16] When it was published it was considered as the largest inorganic anion(!): K. H. Tytko, B. Schönfeld, B. Buss, O. Glemser, *Angew. Chem.* **1973**, *85*, 305 – 307; *Angew. Chem. Int. Ed. Engl.* **1973**, *12*, 330 – 332.
[17] Examples are the transitions from the hypothetical highly negatively charged V^{IV} based Keggin unit to an extended stable one by its capping with six VO^{2+} additional groups,[6,7b] (see also A. Müller et al., *Inorg. Chem.* **1997**, *36*, 5239 – 5250) from a $\{Mo_{57}\}$ cluster to the extended $\{Mo_{63}\}$-type on capping with six MoO^{4+} groups,[18] from the Mo_{176}- to the Mo_{248}-type cluster anion on capping with two neutral $\{Mo_{36}\}$ fragments.[19] A further example refers to remarkable processes occurring during the formation of the unsymmetrical molybdenum oxide based $\{Mo_{37}\}$ cluster: after a highly reduced ε-Keggin-type $\{Mo^{V}_{12}\}$ unit is capped by four electrophilic MoO_3 groups, which are then reduced, the resulting species is capped by the positively charged $\{Mo_{11}\}$ and $\{Mo_{10}\}$ fragments. (In many cases these types of processes cause a decrease of unusual very large negative charges of the intermediates.)[18]
[18] A. Müller, J. Meyer, E. Krickemeyer, C. Beugholt, H. Bögge, F. Peters, M. Schmidtmann, P. Kögerler, M. J. Koop, *Chem. Eur. J.* **1998**, *4*, 1000 - 1006.
[19] A. Müller, S. Q. N. Shah, H. Bögge, M. Schmidtmann, *Nature* **1999**, *397*, 48 – 50.
[20] S. Polarz, B. Smarsly, C. Göltner, M. Antonietti, *Adv. Mater.* **2000**, *12*, 1503 – 1507; S. Polarz, B. Smarsly, M. Antonietti, *ChemPhysChem* **2001**, *2*, 457 – 461; D. Kurth, P. Lehmann, D. Volkmer, A. Müller, D. Schwahn, *J. Chem. Soc. Dalton Trans.* **2000**, 3989 – 3998, and references therein. The cluster material can be handled easily, as it can now be obtained in facile syntheses A. Müller, S. K. Das, E. Krickemeyer, C. Kuhlmann, *Inorg. Synth.*, *34* (Ed.: J. Shapley) in press.
[21] See for instance: a) A. Müller, R. Maiti, M. Schmidtmann, H. Bögge, S. K. Das, W. Zhang, *Chem. Commun.* **2001**, 2126 – 2127; b) G. Mestl, C. Linsmeier, R. Gottschall, M. Dieterle, J. Find, D. Herein, J. Jäger, Y. Uchida, R. Schlögl, *J. Mol. Catal. A* **2000**, *162*, 455 – 484.
[22] J. Haber, L. Lalik, *Catal. Today* **1997**, *(C)33*, 119 – 137; J. Haber "*Molecular mechanism of heterogeneous oxidation—Organic and solid state chemists' views*" in *Studies in Surface Science and Catalysis*, *Vol. 110* (Eds.: B. Delmon, Y. T. Yates), Elsevier, Amsterdam, **1997**, p. 1.
[23] V. E. Henrich, P. A. Cox, *The Surface Science of Metal Oxides*, Cambridge University Press, Cambridge, **1994**.
[24] In this context the presence of (many) O=MoO_6-type pentagonal bipyramids in **1a** which are considered to be responsible for important types of selective oxidations based on molybdenum oxide catalysts[21b] is noteworthy.
[25] See: *Nanotechnology: Research and Perspectives* (Eds.: B. C. Crandall, J. Lewis), MIT Press, Cambridge, **1992**.
[26] See: J. Simon, P. Bassoul, *Design of Molecular Materials: Supramolecular Engineering*, Wiley, Chichester, **2000**.
[27] a) E. Ben-Jacobs, H. Levin, *Nature* **2001**, *409*, 985 – 986; b) H. Haken, A. Wunderlin, *Die Selbststrukturierung der Materie: Synergetik in der unbelebten Welt*, Vieweg, Braunschweig, **1991**; c) D'Arcy Thompson, *On Growth and Form*, Cambridge University Press, Cambridge, **1961** (Canto edition, **1997**); d) A. M. Turing, The chemical basis of morphogenesis, *Philos. Trans. R. Soc. London Ser. B* **1952**, *237*, 37; e) *From Simplicity to Complexity*, *Part II: Information—Interaction—Emergence* (Eds.: K. Mainzer, A. Müller, W. G. Saltzer), Vieweg, Braunschweig, **1998**; d) P. Ball, *The Self-Made Tapestry: Pattern Formation in Nature*, Oxford University Press, Oxford, **1999**.
[28] A remarkable process of symmetry breaking was discussed by L. Addadi and S. Weiner stating in the abstract "*Understanding the formation of asymmetrical shapes during the growth of symmetrical crystalline structures is a first step towards understanding asymmetry in biology*" (L. Addadi, S. Weiner, *Nature* **2001**, *411*, 753 – 755). The authors refer in this context to the Curie symmetry principle[29] (see also [26] where it is considered with respect to supramolecular engineering), which is not fulfilled in the present case, if B is considered as the cause for the "growth" of C.[30]
[29] I. Hargittai, M. Hargittai, *Symmetry through the Eyes of a Chemist*, VCH, Weinheim, **1986**; P. Curie, *J. Phys. (Paris)* **1894**, *3*, 393; see also: I. Hargittai, M. Hargittai, *In Our Own Image: Personal Symmetry in Discovery*, Kluwer, New York, **2000**, p. 216.
[30] It seems reasonable to assume that during the route to **1a** an anion with the approximate shape of B is first formed, which is—because of its much larger hydrophilic surface—more soluble than **1a**.
[31] H. S. M. Coxeter, *Introduction to Geometry*, Wiley, New York, **1989**, pp. 152 – 154.
[32] See ref. [31], pp. 373 – 374.
[33] Given a vertex v in a polyhedral net incident with k distinct polygons, one n_1-, one n_2-, …, and one n_k-gon, its combinatorial curvature is $2 - (n_1 - 2)/n_1 + (n_2 - 2)/n_2 \ldots + (n_k - 2)/n_k$ if that vertex is an interior vertex, and $1 - (n_1 - 2)/n_1 + (n_2 - 2)/n_2 \ldots + (n_k - 2)/n_k$ if it lies on the boundary. If the combinatorial curvature at a vertex v is positive (negative), so is the expected geometric curvature at that vertex for any "reasonable" embedding of the polyhedron in 3-space (e.g. the combinatorial curvature at each of the 60 vertices of the spherically shaped C_{60} polyhedron is easily computed as $2 - (4/6 + 4/6 + 3/5) = 1/15$). Euler's theorem can be rephrased in terms of combinatorial curvatures as stating that their sum, taken over all vertices of a given polyhedron P, is—quite independently of that polyhedron's specific structure—always equal to four if the polyhedron's topology is that of a sphere (e.g. the combinatorial curvature at each vertex of a 60-vertex polyhedron of spherical shape must be 1/15 in the average, and it must be equal to 1/15 whenever all vertices have the same combinatorial curvature) and that it vanishes whenever the polyhedron's shape is that of a torus or that of a *cylinder*, i.e. a body shaped like an open tube with two circular boundary lines while this sum is negative for every polyhedron of higher genus. This implies that every region of a polyhedral net with predominantly positive combinatorial curvature must have the shape of a cap while an area of predominantly negative combinatorial curvature must be saddle shaped. A case in point are *Fowler's Phantasmagorical Fulleroids* (see "Phantasmagorical Fulleroids": A. Dress, G. Brinkmann, *Match* **1996**, *33*, 87 – 100), the two smallest possible fulleroidal structures with icosahedral symmmetry consisting of pentagons and heptagons, only, as depicted in Figure 6a. They illustrate negative curvature inbetween the areas with strong positive curvature. See also [31] for background material and further details.
[34] Note that the sum $240 \times (4/315) + 48 \times (4/315) - 16 \times (30/315) - 24 \times (28/315)$ vanishes as predicted by Euler's theorem.

  1433-7851/02/4107-1167 $ 20.00+.50/0